Separation Science and Technology
Publication details, including instructions for authors and subscription information:
http://www.informaworld.com/smpp/title~content=t713708471

CONSTANT PRESSURE FILTRATION OF MONO-DISPERSED DEFORMABLE PARTICLE SLURRY

Wei-Ming Lu[a]; Kuo-Lun Tung[b]; Shu-Mei Hung[a]; Jia-Shyan Shiau[a]; Kuo-Jen Hwang[c]
[a] Department of Chemical Engineering, National Taiwan University, Taipei, Taiwan, R.O.C. [b] Department of Chemical Engineering, Chung Yuan University, Chungli, Taiwan [c] Department of Chemical Engineering, Tamkang University, Taipei Hsien, Taiwan, R.O.C.

Online publication date: 31 August 2001

To cite this Article Lu, Wei-Ming , Tung, Kuo-Lun , Hung, Shu-Mei , Shiau, Jia-Shyan and Hwang, Kuo-Jen(2001) 'CONSTANT PRESSURE FILTRATION OF MONO-DISPERSED DEFORMABLE PARTICLE SLURRY', Separation Science and Technology, 36: 11, 2355 — 2383
To link to this Article: DOI: 10.1081/SS-100106098
URL: http://dx.doi.org/10.1081/SS-100106098

SEPARATION SCIENCE AND TECHNOLOGY, 36(11), 2355–2383 (2001)

CONSTANT PRESSURE FILTRATION OF MONO-DISPERSED DEFORMABLE PARTICLE SLURRY

Wei-Ming Lu,[1,*] Kuo-Lun Tung,[1,†] Shu-Mei Hung,[1] Jia-Shyan Shiau,[1] and Kuo-Jen Hwang[2]

[1]Department of Chemical Engineering, National Taiwan University, Taipei 106, Taiwan, R.O.C.
[2]Department of Chemical Engineering, Tamkang University, Tamsui, Taipei Hsien 251, Taiwan, R.O.C.

ABSTRACT

Constant pressure filtration experiments of Ca-alginate gel particle, *Saccharomyces cerevisiae*, and polymethyl methacrylate (PMMA) were conducted to study the local properties of cake layer formation by deformable particles. Effects of particle deformation due to frictional drag and cake mass on cake compression and contact area among particles were examined. The factors that lead to the increase in filtration resistance were discussed. The dynamic analysis proposed by Lu and Hwang in 1993 was modified to analyze formation and compression of cake during cake filtration of deformable particle slurry. A thin skin layer of low porosity and high resistance was formed next to the filter medium due to severe de-

*Corresponding author. Fax: +886-2-23623040; E-mail: wmlu@ccms.ntu.edu.tw
†Current address: Department of Chemical Engineering, Chung Yuan University, Chungli 320, Taiwan. E-mail: kuolun@cycu.edu.tw

formation, caused by frictional drag, of the first layer. The results of this study clearly indicate that neglecting the area-contact effect among particles will lead to an overestimate of cake porosity, and neglecting the transient effect of cake compression during gel layer formation will result in an underestimate of cake porosity. The characteristic values of filter cake obtained from dynamic analysis can be used to predict the performance of the filtration of slurries containing deformable particles.

Key Words: Cake filtration; Deformable particle; Filtration; Local cake properties; Particle deformation

INTRODUCTION

Separation of deformable particles from liquid is frequently necessary in biomass processing and chemical/biological waste treatment. The deformation of particles during a separation process complicates the processing of a variety of materials, including gels, blood cells, bacteria, microorganisms, and chemical/biological waste products. Although many materials of industrial interest are deformable when subjected to a hydraulic drag force, a fundamental understanding of the filtration mechanisms of deformable particles remains elusive.

Numerous investigators (1–4) claimed that flow through highly compactible cakes produces a highly nonuniform structure with a tight skin of low porosity next to the supporting medium. This skin layer leads to adverse effects in which increasing filtration pressure has little effect on flow rate or average porosity. Tiller (5) first attempted to develop the theory for compactible cake filtration and proposed a power function to relate the local cake properties with solid compressive pressure. Tiller also interpreted the compressibility of cake by an exponent n defined as the cake compactibility factor. A large value of n represents a more compactible filter cake. Recently, a number of researchers presented different formulations of compactible cake filtration for rigid particle slurry and many investigations have been undertaken of flocculated suspension filtration (6–9). However, in all of these works, the solid particles in flocs were treated as nondeformable.

In many cases, solid particles in the cake migrate and deform as a result of the drag forces associated with the liquid flow. It always results in an erroneous prediction on filtration rate when the conventional cake filtration theory is used. Tosun (10) obtained a simplified solution for one-dimensional, constant-pressure filtration by relating the stress-strain relations for the deformable solid particles with Hooke's law. However, the deformation of a solid network does not necessarily require the deformation of individual solid particles (11). Re-

cently, Jönsson and Jönsson (3) developed a model to describe both static and dynamic behaviors of fluid flow through viscoelastic deformable materials. Meeten (12) regressed the experimental data of filtrate versus time for Sephadex slurry and found that the Ruth equation can only be valid for the case of high septum resistance. However, no information about the cake structure formed by deformable particles has been discussed. Yet, various gel-layer models based on mass transfer theory have been proposed to describe cross-flow filtration for deformable biosolids. Although these models can predict the steady-state flux for some biosolids, the regressive values of the parameters used often result in considerable discrepancies with the physical facts. In addition, no attempt has been made to investigate contact-area variation among deformable particles during the course of cake filtration.

Utilizing the value of the cake surface porosity and a set of filtration data (volume of filtrate per unit medium area (v) vs. filtration time (t) for constant pressure filtration or pressure vs. t for constant rate filtration) to determine the local cake properties has proven to be a reliable method (13–15).

In this study, deformable particles, such as the ca-alginate gel particle and *Saccharomyces cerevisiae* slurries, were used to examine by modified dynamic analysis how the filtration of deformable particle slurries will differ from that of rigid particle slurries. For deformable particles, the filtration equations that were based on point contact were modified to include the effects of area contact and transient compression. The effect of particle deformation due to frictional drag and cake mass on porosity reduction was examined to determine how this effect leads to increased filtration resistance.

THEORETICAL ANALYSIS

During the course of cake filtration of deformable particles, particle deformation due to frictional drag and cake mass will result in area contact among particles and noninstantaneous variation of cake structure. To examine how this variation leads to the decrease of cake porosity and increase in filtration resistance, filtration equations were based on the assumption that point contact must be modified to cover the effects of the area contact and transient compression of particles. The assumptions made are as follows:

1. For simplicity, all particles were assumed to be spherical before compression and deformable without change in volume.
2. The variation of particle shape during cake compression is not attained instantaneously and can be expressed by a viscoelastic model. The viscoelastic constant and retardation time, τ, related to a filter cake are assumed to be constant during filtration.
3. Filtration liquid is incompressible.

MARCEL DEKKER, INC.
270 Madison Avenue, New York, New York 10016

Effective Solid Compressive Pressure in a Cake Composed of Deformable Particles

In the derivation of the drag equations of filtration for rigid particle slurries, particles were assumed to be in point-contact mode and the compression was assumed to attend to an equilibrium instantaneously (5). Under this assumption, the liquid pressure is effective over the entire cross section, and the net force on the total mass within the differential distance, dx, is given by

$$\text{net force} = dF_s + AdP_L. \tag{1}$$

F_s represents the solid compressive force; A stands for cross sectional area of the filter cake; and P_L is the hydraulic pressure. This net force equals the differential mass multiplied by the average acceleration. However, because the acceleration of the solid as it is compressed into the cake and the acceleration of the liquid as it passes through the interstices are so small and can be neglected, Eq. (1) may be reduced as

$$dF_s + AdP_L = 0. \tag{2}$$

If the pseudo-solid compressive pressure P_s is defined as F_s/A, it gives

$$dP_s + dP_L = 0 \tag{3}$$

Integration of Eq. (3) across the entire cake gives

$$P_s + P_L = \Delta P, \tag{4}$$

where ΔP is the applied filtration pressure at the surface of the cake.

If the solid spheres are deformable under compression, the derived equations based on the assumption of point contact should be modified to include the effect of the contact area as shown in Fig. 1. Tiller and Huang (16) analyzed the case for finite contact area and presented an equation that reduced to Eq. (4) when contact area is negligible. In a filter cake composed of deformable particles, an average contact area, A_c, among particles is determined for each control layer of cake, and Eq. (2) should be modified to the form

$$dF_s + (A - A_c)dP_L = 0. \tag{5}$$

By defining the pseudo-solid compressive pressure as the frictional drag divided by cross-sectional area, $P_s = F_s/A$, and integrating across the cross section, the following equation is obtained:

$$P_s + \left(1 - \frac{A_c}{A}\right) P_L = P_s + \Omega P_L = \Delta P, \tag{6}$$

MARCEL DEKKER, INC.
270 Madison Avenue, New York, New York 10016

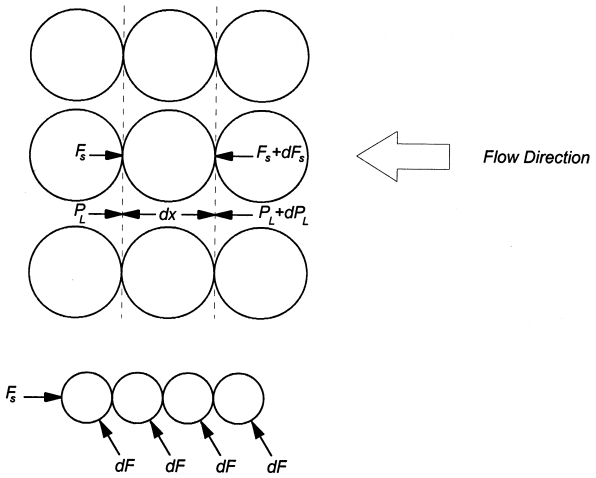

(a) Cake formed by rigid particles

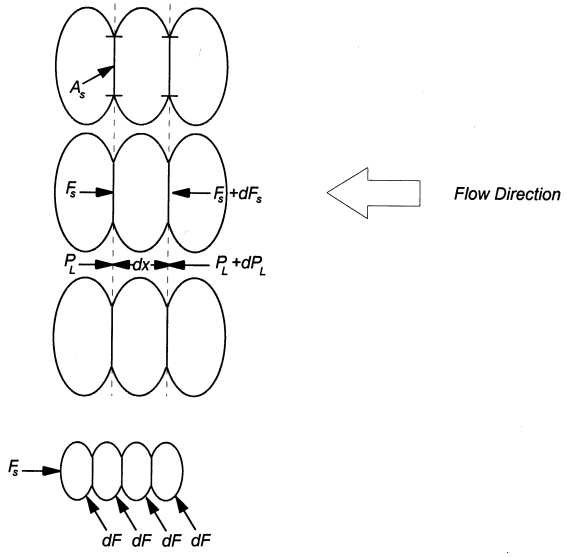

(b) Cake formed by deformable particles

Figure 1. Compressive force due to frictional drag.

MARCEL DEKKER, INC.
270 Madison Avenue, New York, New York 10016

Table 1. The Differences Between Point Contact and Area Models

	Point Contact $A_c = 0, \Omega = 1$	Area Contact $1 - \frac{A_c}{A} = \Omega(\varepsilon)$
Force balance	$P_s + P_L = P$	$P_s(t) + \Omega(t)\, P_L(t) = P$
	$dP_L = -dP_s$	$dP_L(t) = -\left[\frac{P_L(t) \cdot d\ln\Omega(t) + dP_s(t)}{\Omega(t)}\right]$
Darcy's law		
$\frac{dP_L}{dx} = \frac{\mu}{K} q$	$\frac{dP_s}{dx} = -\frac{\mu}{K} q$	$\frac{dP_s(t)}{dx} = \frac{[P - P_s(t)]d\ln\Omega(t)}{dx} - \Omega(t)\frac{\mu}{K} q(t)$
Kozeny's equation		$\frac{dP_s}{dx} = \frac{(P - P_s)d\ln\Omega}{dx} - \Omega k S_0'^2 \frac{(1-\varepsilon)^2}{\varepsilon^3}\mu q$
$\frac{dP_L}{dx} = kS_0^2 \frac{(1-\varepsilon)^2}{\varepsilon^3}\mu q$	$\frac{dP_s}{dx} = -kS_0^2 \frac{(1-\varepsilon)^2}{\varepsilon^3}\mu q$	$= \frac{(P - P_s)d\ln\Omega}{dx} - \Omega^3 k S_0^2 \frac{(1-\varepsilon)^2}{\varepsilon^3}\mu q$
		where $S_0' \cong S_0\left[1 - \frac{A_c}{A}\right] = S_0 \cdot \Omega$

which reduces to Eq. (4) when $A_c/A = 0$, *i.e.*, the assumption of point contact. The differences of force balance equations, Darcy's and Kozeny's equations, between point contact and area contact are summarized in Table 1.

Effective Specific Surface Area in a Deformable Particles Bed

Little research has been done into the study of the packed structure of soft or deformable materials where area contact is appreciable. Fischmeister, Arzt, and Olsson (17) studied the development of contact facets between particles during compaction of mono-sized spherical bronze powder and illustrated the variation of contact area between deformed particles as a function of porosity. In 2001, Lu et al. (18) studied the relation between contact-area ratio and porosity of a Ca-alginate particle bed under uniaxial compression and found that the relation can be expressed as

$$\frac{S_o'}{S_o} = \frac{1 - \exp[-b\varepsilon(t)]}{1 + a\exp[-b\varepsilon(t)]} = 1 - \frac{A_c}{A}, \tag{7}$$

where ε is the cake porosity, S_o is the specific surface area of the particles before compression; S_o' is the effective specific surface area of the particles after compression; and a and b are the viscoelastic properties of the gel-particle bed. The parameters of a and b can be obtained according to quantitative metallography. The compressed gel particles were notched by a saw and fractured. The flattened particle contacts were revealed by lineal analysis. The experimental determined values of a and b for the various kinds of particles used in this study are listed in Table 2.

MARCEL DEKKER, INC.
270 Madison Avenue, New York, New York 10016

Table 2. The Values of a and b for Various Particles

Types of Particle and Packing	a	b
S cerevisiae	17.35	13.75
Ca-Alginate (0.50%)	25.00	15.00
Ca-Alginate (0.75%)	5.50	11.00
Ca-Alginate (1.00%)	3.00	10.00

A Model for Transient Compression of Filter Cake

Because the equilibrium porosity will not be attained instantaneously for filter cake formed by deformable particles, a viscoelastic model may be used to express the instantaneous variation of cake porosity during cake compression:

$$\frac{\varepsilon_t - \varepsilon_i}{\varepsilon_f - \varepsilon_i} = 1 - \exp\left(\frac{-t}{\tau}\right), \tag{8}$$

where ε_i is the local cake porosity before compression ($t = 0$); ε_f is the local cake porosity at equilibrium after compression ($t \to \infty$); ε_t is the local cake porosity at time t; and τ is the retardation time. As shown in Fig. 2a, for a nontrivial value of τ, the equilibrium cake porosity, ε_f, is not attained instantaneously for filter cake formed by deformable particle, while as $\tau = 0$, the local cake porosity reaches the equilibrium value, ε_f, from the initial value of ε_i instantaneously. Figure 2a also depicts that the larger the value of τ, the more time will be needed for cake poros-

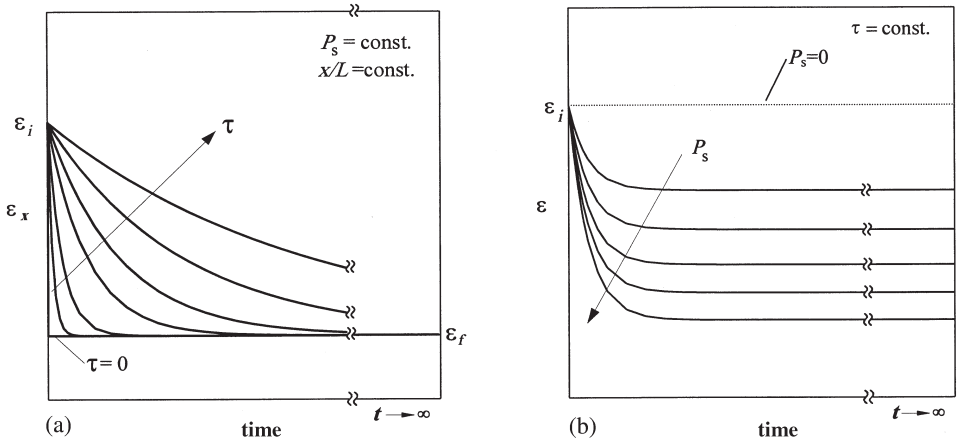

Figure 2. (a) ε vs. t., (b) Transient variation of ε_x.

MARCEL DEKKER, INC.
270 Madison Avenue, New York, New York 10016

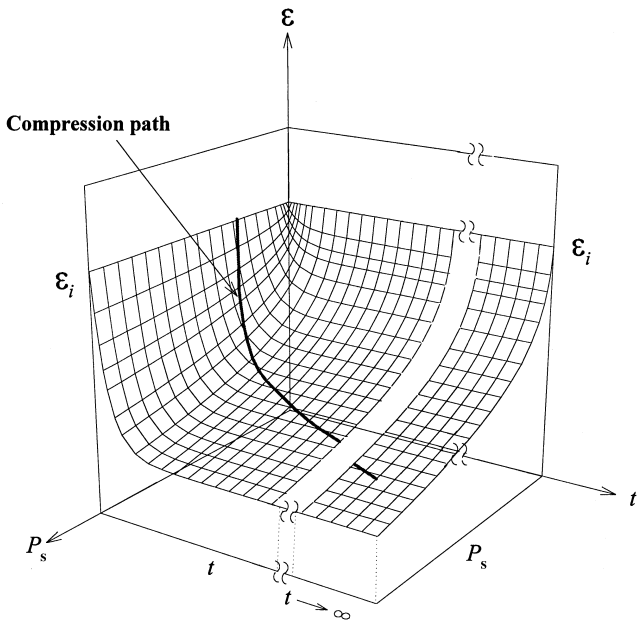

Figure 3. Transient behavior of cake compression.

ity to reach equilibrium ε_f. However, an increase of the solid compressive pressure will result in a decrease of equilibrium cake porosity, ε_f, as illustrated in Fig. 2b. Figure 3 shows schematically the P_s-ε-t surface that represents the compression state of filter cake with a nontrivial constant value of τ in a filtration system. The compression path curve represents the variation of cake porosity with respect to time at a specified location in a filter cake composed of deformable particles.

Continuity Equation for a Cake Under Compression

For a specified controlled mass (each layer of the cake), the continuity equation of compression is (19)

$$\left(\frac{\partial q}{\partial x}\right)_t = \left(\frac{\partial \varepsilon}{\partial t}\right)_x. \tag{9}$$

This equation can be employed to describe the relationship between the change of the filtrate flow rate and the variation of cake porosity.

In this study, it is assumed that no interlayer transport of particles occur; *i.e.,* a cake layer may be compressed, but no transport of particles out of or into the

Marcel Dekker, Inc.
270 Madison Avenue, New York, New York 10016

layer occurs, as shown in Fig. 4. Under this assumption, the value of $\Delta x(1-\varepsilon)$ of cake layer j remains constant during filtration; thus, the relationship between cake thickness and its porosity before and after compression can be represented as

$$\frac{\Delta x_{t+\Delta t}}{\Delta x_t} = \frac{(1-\varepsilon)_t}{(1-\varepsilon)_{t+\Delta t}}. \tag{10}$$

Through solutions of Eqs. (9) and (10), the variations of the cake porosity and the filtrate flow rate within the cake layer can be estimated.

Local Specific Filtration Resistance

The well-known Kozeny equation for fluid flow through a porous medium can be expressed as

$$q = \left(\frac{dP_L}{dx}\right) \frac{\varepsilon^3}{\mu k (S_o')^2 (1-\varepsilon)^2} \tag{11}$$

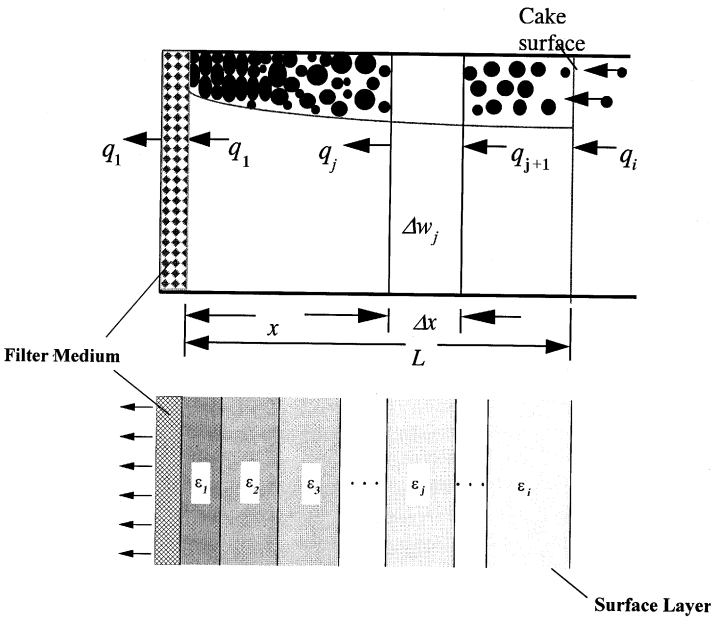

Figure 4. A schematic diagram of control mass in filter cake. q is the filtration rate (m^3/m^2s).

in which ε is the cake porosity; μ is the viscosity of the fluid; S'_o is the effective specific surface area of the particles after compression and k is the Kozeny constant. Happel and Brenner (20) derived an expression for the relationship between the Kozeny constant and porosity:

$$k = \frac{2\varepsilon^3}{(1-\varepsilon)\{\ln[1/(1-\varepsilon)] - [1-(1-\varepsilon)^2]/[1+(1-\varepsilon)^2]\}}. \tag{12}$$

Thus, prior to applying Eq. (11) to estimate the filtrate flow rate or the pressure drop through a differential layer of filter cake, the value of k should be corrected using the local cake porosity. If the porosity is smaller than 0.35, the Kozeny constant can be modified according to the correlation results of Sparrow and Loeffler (21), such as

$$k = 1.75 \times \tan[1.25 \times (2\varepsilon - 1)] + 3.65. \tag{13}$$

This equation can be used suitably for the cases in which cake porosities range from 0.4 to 0.1.

Comparing Eq. (11) with the differential form of the cake filtration equation, the specific filtration resistance in the cake can be given as

$$\alpha = k(S'_o)^2 \frac{(1-\varepsilon)}{\rho_s \varepsilon^3}. \tag{14}$$

To perform a dynamic analysis on cake formation and compression during the course of filtration, some knowledge of conditions is required.

The Known Conditions

The conditions of the system required to undertake the analysis on cake and compression are summarized as follows:

1. Flow rate of filtrate, q_1. The instantaneous flow rate of filtrate can be obtained by differentiating the total received filtrate volume per unit area with respect to time.
2. Flow rate of fluid at cake surface, q_i. When the mass balance is taken for the whole filter cake, the ratio of the fluid flow rate at the cake surface, q_i, to the flow rate of the filtrate, q_1, can be expressed as

$$\frac{q_i}{q_1} = \frac{\left\{(1-s)\left(1-\varepsilon_{av}-L\frac{d\varepsilon_{av}}{dL}\right) - s(m_i-1)(1-\varepsilon_i)\right\}(1-\varepsilon_{av})}{\left[(1-m\cdot s)\left(1-\varepsilon_{av}-L\frac{d\varepsilon_{av}}{dL}\right)(1-\varepsilon_{av}) - sL\frac{\rho}{\rho_s}\frac{d\varepsilon_{av}}{dL}\right]}, \tag{15}$$

where s is the mass fraction of particles in the slurry, and m and m_i are the mass ratios of wet to dry cake of the whole cake and on the cake surface, respectively (22).

MARCEL DEKKER, INC.
270 Madison Avenue, New York, New York 10016

3. Porosity on cake surface, ε_i. The cake surface porosity can be obtained by means of a low head filtration system as proposed by Haynes (22).
4. Filter medium resistance, R_m. In a cake filtration, the pressure drop through the filter medium, ΔP_m, cannot be neglected. If the resistance of the filter septum, R_m, remains constant during the course of filtration, then the value of R_m can be obtained by extrapolation of the filtration data through the equation

$$R_m = \frac{P \mid_{t=0}}{(q_1 \mid_{t=0} \cdot \mu)}.$$

Then, the pressure drop of the fluid flow through the filter medium can be calculated accordingly.
5. Mass of instantaneous cake formation, Δw_i. The mass of cake formed within a very short period can be estimated by (22)

$$\Delta w_i(t) = \frac{\rho s}{1 - ms}\left[\frac{dv}{dt} + \frac{sv}{1 - ms}\frac{dm}{dt}\right]\Delta t. \tag{16}$$

6. Cake thickness. Because the instantaneous equilibrium cannot be reached for the cake formed by deformable particles and instantaneous cake thickness is needed for dynamic analysis, it can be measured by an optical in situ measurement technique that is described in the experimental section.

Procedure to Analyze Cake Properties During a Filtration

Based on the above equations and the known conditions, a dynamic simulation process was established for estimating the variations of local cake properties and the formation of filter cake during the course of filtration. In the simulation, the differential equations described in the previous section were solved using a backward difference numerical scheme. The local hydraulic pressure, the local porosity, the local specific filtration resistance, the contact area between particles within a filter cake, and the viscoelastic properties of filter cake can be analyzed dynamically along a filtration process like that illustrated in Fig. 5. The simulation was performed for several trial loops of various trial values of τ instead of one loop ($\tau = 0$) as in the work of Lu, Huang, and Hwang for rigid particle slurry filtration (14). The detailed procedures are described as follows:

1. Input the values of ε_i, L_e, R_m, and a set of v vs. t data from a constant pressure filtration test.
2. To obtain the equilibrium value of porosity, ε_f, of each layer, a trial value of $\tau = 0$ was adopted in the following steps in the first simulation loop ($l = 1$).

MARCEL DEKKER, INC.
270 Madison Avenue, New York, New York 10016

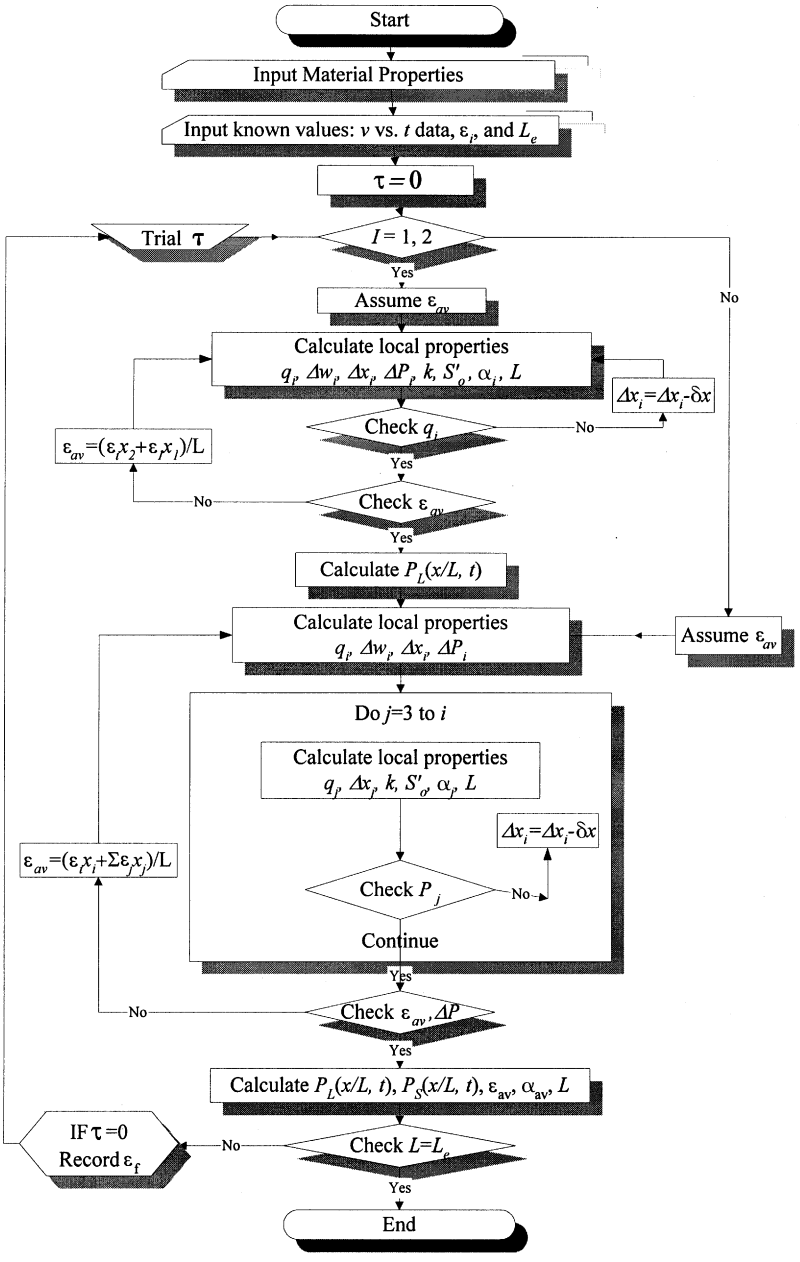

Figure 5. Flow diagram of simulation procedure for constant-pressure filtration of deformable particles.

MARCEL DEKKER, INC.
270 Madison Avenue, New York, New York 10016

3. At the beginning of filtration, the first-formed layer of cake on the filter medium has not been compressed yet, and the cake porosity, $\varepsilon_1|_{t_1}$, is equal to ε_i. The values of $\Delta w_i|_{t_1}$ could be calculated by Eq. (16). The values of $k_1(S'_{o,1})^2|_{t_1}$, $k_1|_{t_1}$ and $\alpha_1|_{t_1}$ in this first cake layer could be calculated by Eqs. (11), (12), and (14), respectively.
4. When a new layer of cake has been formed on the cake surface, the lower cake may be compressed. The values of $\Delta w_i|_{t_2}$ could be calculated by Eq. (16). In the first loop of $l = 1$, the new thickness of the lower cake layer can be expressed as $\Delta x_1|_{t_2} = \Delta x_1|_{t_1} - \delta x$, where δx is the thickness change due to compression; thus, the whole cake thickness can be estimated by $L|_{t_2} = \Delta x_2|_{t_2} + (\Delta x_1|_{t_1} - \delta x)$. The use of an infinitesimal value of δx to calculate the value of $d\varepsilon_{av}/dL$ by $(\varepsilon_{av}|_{t_2} - \varepsilon_{av}|_{t_1})(L|_{t_2} - L|_{t_1})$ allows one to use Eq. (15) to calculate the flow rate of liquid at the cake surface, $q_i|_{t_2}$ (or $q_2|_{t_2}$). The pressure difference across the newly formed layer of cake, $\Delta P_2|_{t_2}$, can be calculated by Eq. (11), and the pressure drop across the lower layer of cake can be calculated by $\Delta P_1|_{t_2} = \Delta P - \Delta P_2|_{t_2}$.
5. In the first loop of $l = 1$, substituting the trial value, δx, into Eq. (10) to estimate $\varepsilon_1|_{t_2}$ of the lower layer of cake enables one to use Eq. (7) to calculate the values of $S'_{o,1})|_{t_2}$. The value of $k_1|_{t_2}$ could be calculated either by Eq. (12) or by Eq. (13), depending on the value of porosity. Then, the value of $q_1|_{t_2}$ could be estimated by Eq. (11). Repeat this iteration until the calculated value of $q_1|_{t_2}$ converges to the experimental value of $q_1|_{t_2}$. After the local properties of the bottom and surface layers have been calculated, the average porosity of the entire cake can be recalculated by

$$\varepsilon_{av}|_{t_2} = \left[\frac{(\varepsilon_1\Delta x_1 + \varepsilon_2\Delta x_2)}{(\Delta x_1 + \Delta x_2)}\right]\Bigg|_{t_2}.$$

The calculated values should be substituted back to step 4 until the residue of the calculated value of $\varepsilon_{av}|_{t_2}$ is less than 1×10^{-3}. The solid compressive pressure drop can then be calculated by Eq. (6) instead of Eq. (4).
6. For the following time increment, the values of Δw_i, Δx_i, and q_i could be calculated by using the procedures described in step 4, and using procedures similar to those outlined in step 5, the values of ε_j, α_j, and q_j can be estimated for the jth layer of cake by Eqs. (10), (14), and (9), respectively. After these values are obtained, the pressure distribution and the average cake porosity can be calculated.
7. Repeat the iteration in step 6 until the new calculated pressure distribution matches the pressure distribution in the last iteration and the ΔP equals the known applied pressure.

MARCEL DEKKER, INC.
270 Madison Avenue, New York, New York 10016

8. Repeat steps 6 to 7 until a specified filtration time or filtrate volume is reached. Finally, a set of the equilibrium values of porosity, ε_f, of each layer can be obtained.
9. In the subsequent loops of $l > 1$, because the equilibrium value of porosity, ε_f, of each layer has been obtained in the first loop, the analyzing procedure begins with a nontrivial initial trial value of τ.
10. In each time interval, the mass of instantaneous formed layer on the cake surface and the porosity of the cake layer could be calculated by Eqs. (16) and (8), respectively. Then the values of $S'_{0,1}|_{t_i}$ could be calculated by Eq. (7). The value of $k_1|_{t_i}$, depending on the value of porosity, could be calculated either by Eq. (12) or by Eq. (13). The value of $q_1|_{t_i}$ could be estimated by Eq. (11). Repeat steps 6 to 7 until a specified filtration time or filtrate volume is reached. The trial of τ values is continued until the simulated cake thickness at the end of simulation meets the predetermined experimental value, L_e. Finally, the variations of local cake properties can be simulated for the entire course of the cake filtration.

EXPERIMENTAL

Experimental Apparatus and Procedure

A schematic diagram of the experimental apparatus used in this work is shown in Fig. 6. The slurry was thoroughly agitated in the slurry tank with a magnetic rotor and was pumped into the pressure filter by compressed air. The stainless steel filter chamber had a filtration area of 0.0046 m^2. The filtration pressure was applied to the system through compressed air that was controlled by a pressure regulator. The weight of filtrate was detected by an electronic balance and recorded on a personal computer. The recorded filtration data, e.g., v vs. t, was used to simulate the growth and compression of cake during the filtration. An optical in situ technique by reflection-type photointerrupter was adopted to measure the dynamic cake thickness during each cake filtration experiment (23). Variations of cake thickness were recorded with an accuracy of 10 μm by the transverse value of voltage signal.

Material

In this study, constant pressure filtration experiments of slurries that contained calcium-alginate particles or *S. cerevisiae* were conducted to examine the local properties of a cake layer formed by deformable particles and were

MARCEL DEKKER, INC.
270 Madison Avenue, New York, New York 10016

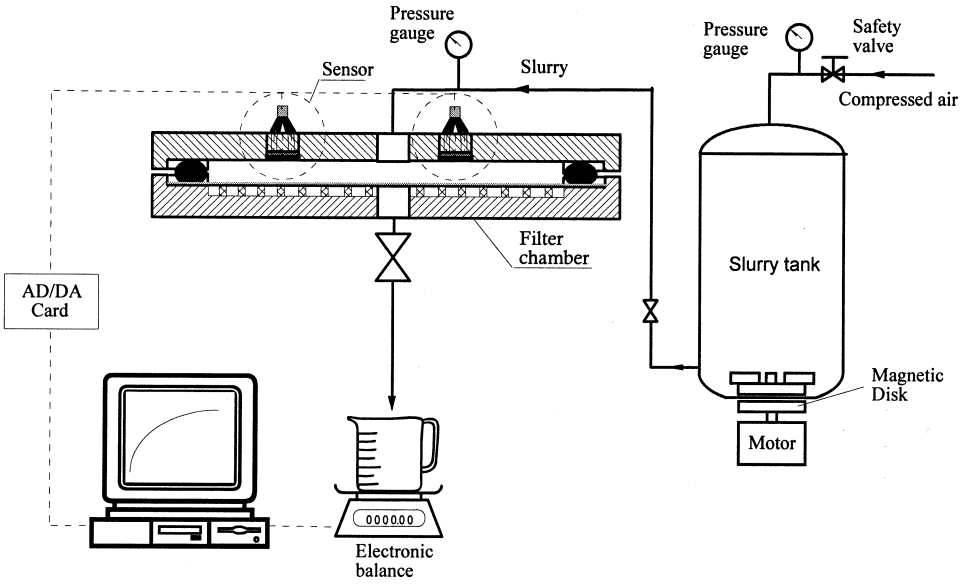

Figure 6. A schematic diagram of constant-pressure filtration apparatus.

compared with the cake formed by PMMA particles, which are considered rigid sphere particles. Ca-alginate particles, treated with 0.02 (wt/wt)% glutaraldehyde, with an average diameter of 5.242 μm (SD = ± 1.544 μm), and with a density of 1070 kg/m^3, were prepared as a slurry with a concentration of 0.2 (wt/wt)%. The Ca-alginate particles were prepared by dosing 0.5, 0.75, or 1.0% sodium alginate solution into a 0.1 mol/L $CaCl_2$ solution from a spraying nozzle to achieve different degrees of particle deformation. *S. cerevisiae* was used as another deformable particle purchased from Sigma Chemical Co, Ltd and suspended in 0.15 mol/L NaCl solution (physiological saline). The average diameter of *S. cerevisiae* was 4.873 μm (SD = ± 0.673 μm). To prevent the breakdown *S. cerevisiae* spores into physiological saline solution, which would change the size distribution of particles in slurry, each run of the experiment, including suspension, agitation, and filtration, was finished in 6 h (24). Water content constitutes the major difference between rigid and deformable particles; the deformable particle contains a lot of water. The water contained in deformable particles should be taken into consideration in dynamic analysis. The water in the total mass of Ca-alginate and *S. cerevisiae* particles amount to 87.3 and 52.0%, respectively. The PMMA particle is a rigid sphere with an average diameter of 5.15 μm (SD = ± 1.103 μm). It has a slightly negative charge and is highly dispersible. It was suspended into deionized water for filtration experiments and the suspension was treated for 30 min with ultrasonic waves for complete dispersion.

RESULTS AND DISCUSSION

Filtration Behavior of Deformable Particles

From constant pressure filtration experiments on a surface filter, the dependence of v on t was described closely by a parabolic profile, i.e. a linear profile in a t/v vs. v plot for various industrial slurries (25). A comparison of dt/dv vs. v plots between rigid and deformable particle slurries under constant pressure in a filtration operation are depicted in Fig. 7. From enlarged and compressed plots shown in Fig. 7, one can see that constant pressure filtration of PMMA slurry shows a perfect linear profile in the dt/dv vs. v plot, which indicates a Ruth behavior, while constant pressure filtration of deformable Ca-alginate particles and *S. cerevisiae* show a nonlinear behavior in dt/dv vs. v plots. The discrepancy of filtration behavior between rigid and deformable particles will be further discussed in the subsequent sections that address the local variation of cake properties.

Figure 8a shows the comparison of the plot of dt/dv vs. v data for deformable Ca-alginate particles of various strengths, and the deformable particles

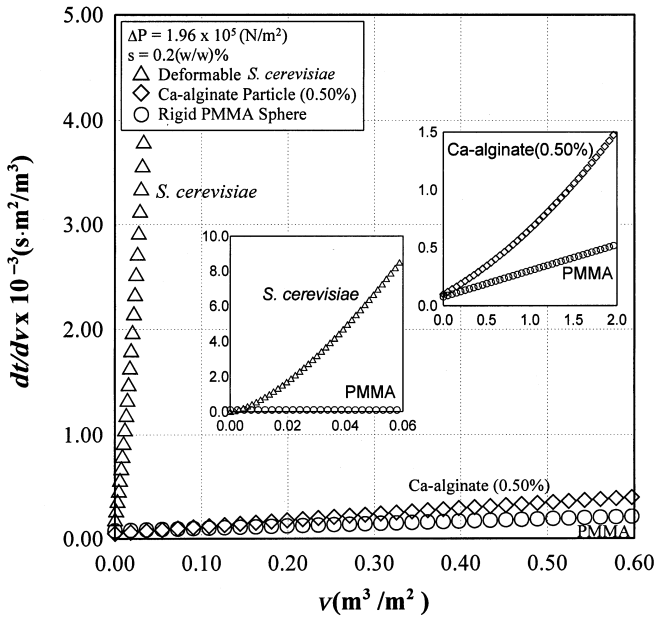

Figure 7. Comparison of dt/dv vs. v data between rigid and deformable particles under constant filtration pressure.

MARCEL DEKKER, INC.
270 Madison Avenue, New York, New York 10016

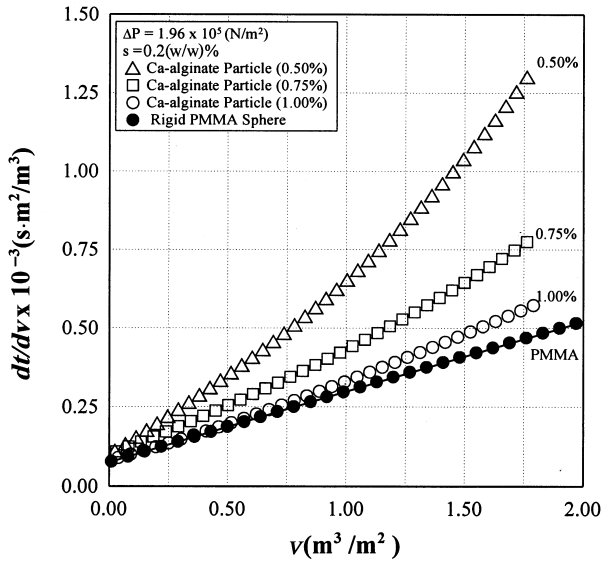

(a)

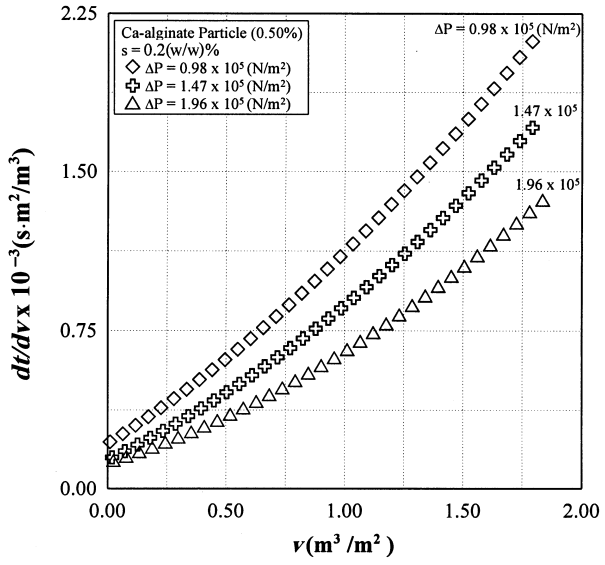

(b)

Figure 8. *dt/dv* vs. *v* of deformable Ca-alginate particle slurry.

are compared with the rigid PMMA particles. All the Ca-alginate gel particle slurries show non-Ruth behavior. Increase of the strength of Ca-alginate particles, *i.e.* increase of the concentration of Na-alginate, will result in a smaller deviation from Ruth behavior because the increased gel particle strength makes it more resistant to deform.

In Fig. 8b, Ca-alginate particle plots are given for various operating pressures. The results imply that the increase in filtration pressure will result in more deformation and greater deviation from Ruth behavior, *i.e.* a more curved profile, which implies larger area contact among the particles.

Figure 9a depicts the growth of cake thickness during filtration for various strength particle slurries under specific constant operation pressure. At the very beginning of filtration or before the thicker cake is formed, the thickness of the cake growth almost follows the same path regardless of particle strength. However, once the particles in the first-formed layer are deformed due to the frictional drag originated from the upper layer particles, the rate of growth will slow down and the growth difference will be shown according to particle strength.

Figures 8a and 9a indicate that the thickness of the cake growth does not depend on particle strength before the thicker cake is formed; however, as shown in Fig. 8a, the profile in the dt/dv vs. v plot largely depends on particle strength in this period. This dependence on particle strength is mainly due to filtration resistance of cake layer, which is proportional to $(1 - \varepsilon)/\varepsilon^3$ according to Eq. (14); for a cake layer with an initial porosity of 0.4, a 10% reduction of layer thickness will result in a 25% structure compaction and will cause at least a 3-fold increase in filtration resistance. Further reduction of cake porosity will accelerate increased filtration resistance. Thus, the cake layer thickness variation is less dependent on the strength of the particles than filtration resistance. In Fig. 9b a cake thickness vs. filtration rate plot for various operating pressures for the softest particle slurry is shown. The paths of cake growth differ from the very beginning of filtration for various operating pressures. A high operation pressure gives more deformation and results in a thinner layer, which results in slower growth of cake thickness.

Empirical Equations for Filter Cake Composted with Deformable Cake

Because the compression of the deformable particle cake cannot be assumed to be completed instantaneously as the rigid particle cakes, the porosity and the specific filtration resistance can no longer be expressed by a unique function of P_s. A set of empirical equations that consists of effects of solid compression pressure and viscoelastic constant, retardation time (τ),

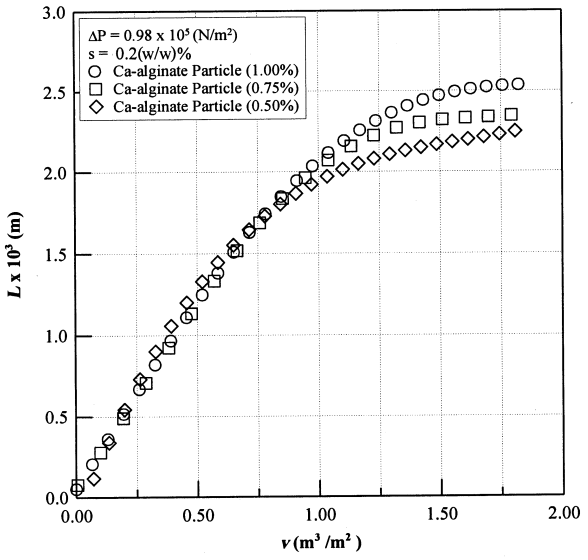

(a)

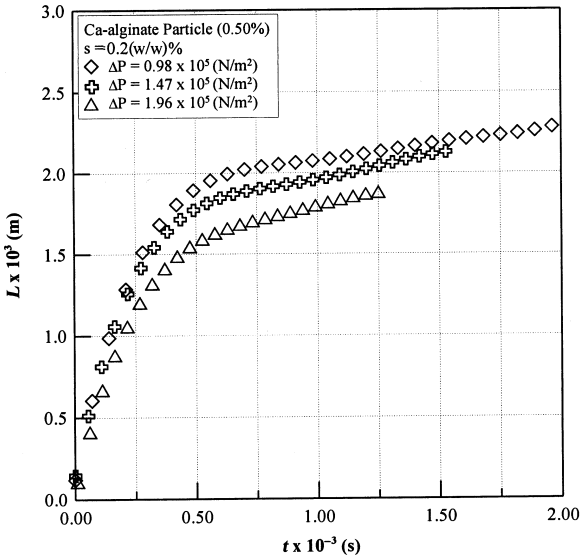

(b)

Figure 9. The cake thickness vs. filtration rate.

is proposed to estimate the values of local cake porosity and specific filtration resistance:

$$1 - \varepsilon_x = (1 - \varepsilon_i)\left\{1 + \left[\left(1 + \frac{P_s}{P_a}\right)^{\beta} - 1\right]\cdot(1 - e^{-\frac{t}{\tau}})\right\} \tag{17a}$$

$$\alpha_x = \alpha_o\left\{1 + \left[\left(1 + \frac{P_s}{P_a}\right)^{n} - 1\right]\cdot(1 - e^{-\frac{t}{\tau}})\right\} \tag{17b}$$

Where the values of parameters n and β are compressibility coefficients and τ is the retardation time. As a general rule, we assumed that $n = 4\beta$ in this study. Here, the viscoelastic constant, retardation time τ, of a filter cake is assumed to be a constant for the sake of simplicity. The values of parameter n, β, and τ can be obtained from dynamic analysis and shown, as in Table 3, as a set of constant pressure filtrations data. The larger the value of τ, the more time is needed to reach the equilibrium cake porosity, ε_f.

Example of Dynamic Analysis

Once ε_i, L_e, and a set of v vs. t are available, one can proceed with the dynamic analysis to obtain details of the course of cake growth. Several examples analyzed for Ca-alginates and *S. cerevisiae* are provided.

Contact Area Between Deformable Gel Particles

Figure 10 depicts the variation of the local contact-area ratio among Ca-alginate particles in a filter cake during the course of filtration. The contact-area ratio is calculated through the use of Eq. (7), which was obtained by the authors' previous work (18). For constant pressure filtration of Ca-alginate particles at an operating pressure of 9.8×10^4 Pa, the contact-area ratio increases from 0 to 0.35 from the cake surface during the progressive deformation of Ca-alginate particles.

Table 3. Characteristic Values of Filter Cakes

Type of Particle	τ(s)	n	β	ε_i	α_o (m/kg)	P_a (kPa)
PMMA	0.23	0.18	0.045	0.478	4.1×10^{10}	2.5
Ca-Alginate (1.00%)	347.5	0.54	0.135	0.495	8.6×10^{10}	2.1
Ca-Alginate (0.75%)	486.2	0.65	0.151	0.500	1.2×10^{11}	2.1
Ca-Alginate (0.50%)	752.1	0.77	0.188	0.501	2.1×10^{11}	2.1
S. cerevisiae	2324.1	0.92	0.255	0.390	6.9×10^{11}	1.21

MARCEL DEKKER, INC.
270 Madison Avenue, New York, New York 10016

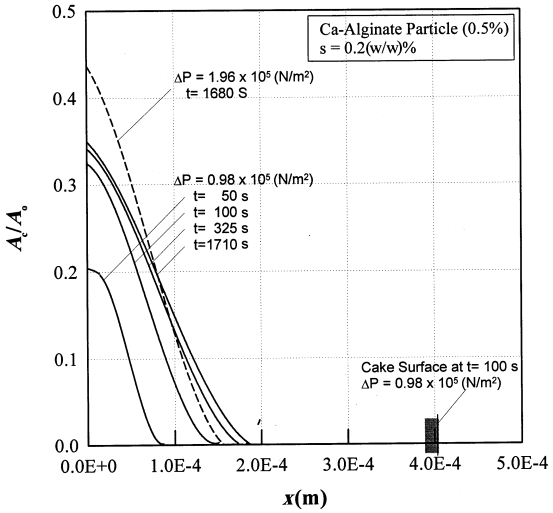

Figure 10. A_c/A_o vs. x for constant-pressure filtration of deformable Ca-alginate particle slurry.

This result indicates that the cake layer is deformed along the cake layer as the effective solid compressive pressure increases through the cake layer to the bottom. The increased operating pressure that results in serious particle deformation and the resulting increase in contact area is shown by a dashed line in Fig. 10.

Solid Compressive Pressure Distribution in Filter Cake

Figure 11 shows the simulated variation of solid compressive pressure distribution during the course of constant pressure filtration as a function of x/L. The diagonal straight line represents incompressible cake structure. Because the rigid particles of incompactible cake will not be rearranged or deformed during cake formation, the structure and local cake porosity is uniform during the course of filtration. For compactible cake, the cake composted with deformable particles, apparent creep effect was observed. At the beginning of filtration, the solid compressive pressure increased gradually toward the filter medium. As the filtration proceeded, the solid compressive pressure built more quickly near the medium-cake interface. Figure 11 shows that almost no variation of solid compressive pressure was found in a majority of the upper region of the filter cake ($x/L > 0.3$) at $t = 1710$ s and 80% of solid compressive pressure drop in the region of 10% of cake near the filter medium. Figure 11 also depicts that increasing the filtration time will further narrow the thickness of skin. That means the compressibility of

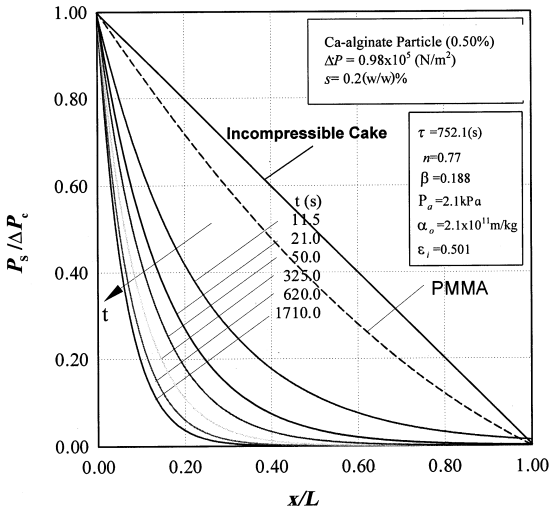

Figure 11. Variation of solid compressive pressure distribution during constant-pressure filtration.

cake will increase during cake formation. That is quite different from the mechanism of cake formation of rigid particles which converge very quickly to a final pressure during the course of filtration.

Porosity and Specific Filtration Resistance in Filter Cake

In Fig. 12, analyzed results of local porosity distributions for Ca-alginate (0.5%) were shown for various time intervals. This figure shows that 60% of cake filtration from the cake surface has almost the cake structure, and a sharp decrease of local cake porosity toward the filter medium can be observed. Results show that as the cake formed by deformable gel particles, a rapid increase in flow resistance or decrease in porosity was created due to area contact between particles, and a thin high-resistance layer was formed next to the filter medium during filtration. Results also show that neglecting the transient effect of cake compression during gel layer formation will result in an underestimate of cake porosity.

Figure 13(a) illustrates the simulated average porosity of cake layer for both nondeformable PMMA particles and deformable Ca-alginate particles. For the case of Ca-alginate particles, the average porosity decreases with time at the beginning because the Ca-alginate particles are deformed in cake layer under applied stress; the deformation results in a tight skin layer. Then the average porosity increases gradually when this effect would not result in further decreased cake porosity, and the forthcoming particles form a loose cake. This phenomenon can

be certified by such an inconceivable low porosity value of 0.1 next to the supporting medium (Fig. 12). A minimum value of average porosity can be found for cake composed of Ca-alginate particles, while a minimum value is not observed for PMMA-particle cake. The discrepancy between cake types is mainly due to different level of particle deformability.

Figure 13b depicts the comparison results of ε_{av} vs. t from a dynamic simulation based upon point-contact mode for rigid particles and area-contact mode for deformable *S. cerevisiae* particles. Results show that neglecting the area-contact effect between particles will lead to an overestimate of cake porosity.

Figure 14 shows the variation of local specific filtration resistance under the same filtration conditions as those depicted in Fig. 12. This figure shows that the values of specific filtration resistance increased toward the filter septum; this result is due to the decrease of porosity near the septum. Also, a thin high-resistance skin layer is formed next to the filter medium due to severe deformation caused by frictional drag at the early stage of filtration. Then, the deformed first layer attenuates the filtration rate and constrains the deformation of subsequent cake layers.

Prediction of Filter Cake Performance Based on Obtained Cake Properties

To examine local cake properties through dynamic analysis, the obtained sets of ε vs. P_s and α vs. P_s data for deformable particles were used in Eqs. (17a)

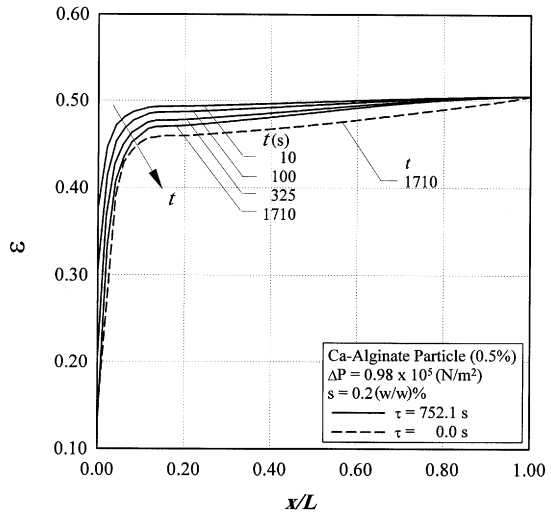

Figure 12. Variation of local cake porosity distribution during constant-pressure filtration.

MARCEL DEKKER, INC.
270 Madison Avenue, New York, New York 10016

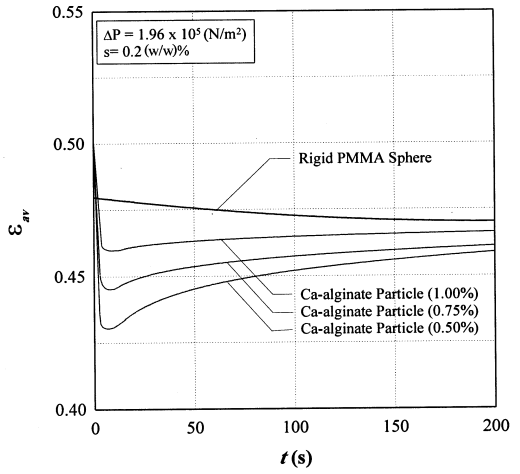

(a)

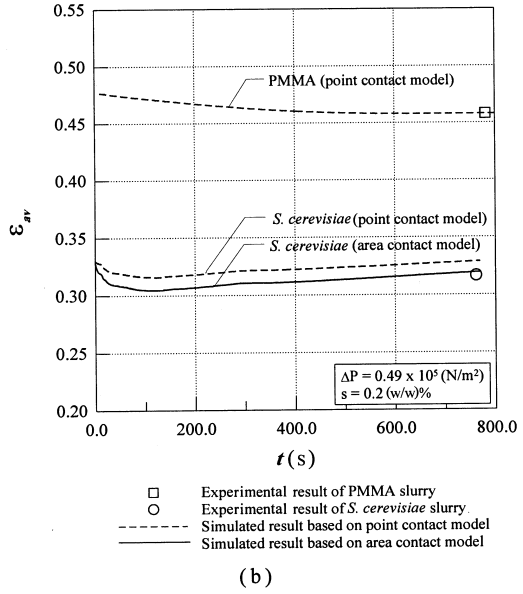

(b)

Figure 13. ε_{a_v} vs. t for constant pressure filtration.

and (17b) to predict filtration performances. The values of parameter n, β, and τ obtained by dynamic analysis of constant pressure filtrations are listed in Table 3. In Fig. 15, the simulated results of constant pressure filtration of deformable Ca-alginate particles are compared with the experimental data. The results show

MARCEL DEKKER, INC.
270 Madison Avenue, New York, New York 10016

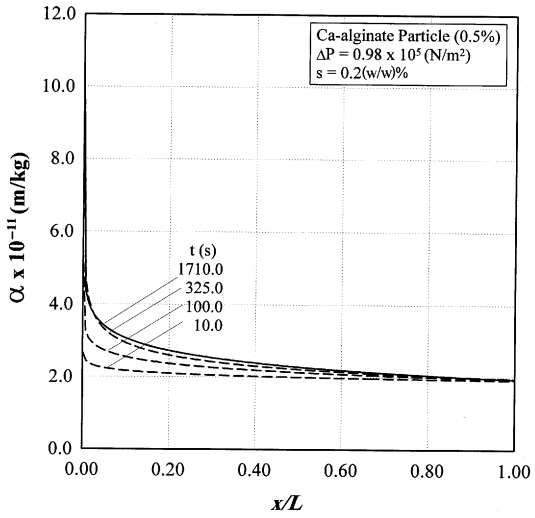

Figure 14. Variation of local specific filtration resistance distribution during constant-pressure filtration.

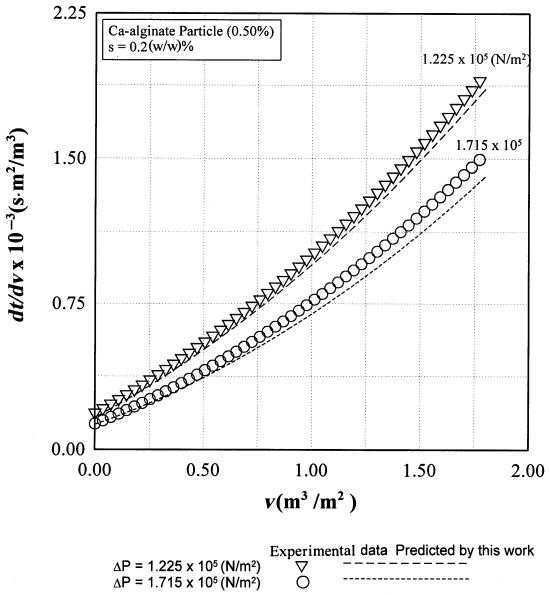

Figure 15. The predicted relation of dt/dv vs. v in constant-pressure filtration by dynamic analysis results and experimental data for Ca-alginate (0.5%).

MARCEL DEKKER, INC.
270 Madison Avenue, New York, New York 10016

that the data obtained from dynamic analysis can provide a good prediction with an average deviation of approximately 6% for low applied pressure to 10% for high applied pressure. Results show a lower profile of predicted dt/dv vs. v curves, *i.e.,* an overestimate of the predicted quantities of filtrate during a filtration course. The prediction error is mainly due to the assumption that the retardation time was always constant in the filter cake during cake formation. In the dynamic analysis, the retardation time constant τ is a trial value, and the checking point is set at the end of filtration, which will result in an underestimate of the value of τ and further causes an underprediction of the cake resistance, which results in an overestimate of filtrate volume and a less curved profile of dt/dv vs. v curves.

CONCLUSIONS

In this study, constant pressure filtration experiments of Ca-alginate gel particle, *S. cerevisiae*, and PMMA were conducted to study the local properties of cake layer formed by deformable particles. Effects of particle deformation due to frictional drag and cake mass on cake compression and contact area among particles were examined, and factors that will lead to the increase in filtration resistance were discussed. A modified dynamic analysis was proposed to analyze cake formation and compression during filtration of deformable particle slurry by taking the area contact among particles and transient deformation of particles into consideration. Results showed that a thin skin layer of low porosity and high resistance is formed next to the filter medium due to deformation of the first layer during filtration and clearly indicate that neglecting the area-contact effect among particles will lead to an overestimate of cake porosity. In addition, neglecting the transient effect of cake compression during gel layer formation will result in underestimated cake porosity. The results show that the characteristic values of filter cake obtained from dynamic analysis for filtration can be used to predict the performance of the filtration of slurries containing deformable particles with an average deviation of less than 10%.

NOMENCLATURE

a	fitted constant adopted in Eq. (7)
A	cross-sectional area of filter cake (m^2)
A_c	averaged contact area among particles in each cake layer (m^2)
b	fitted constant adopted in Eq. (7)
F_s	solid compressive force (N)
k	Kozeny constant
l	the lth loop of simulation

MARCEL DEKKER, INC.
270 Madison Avenue, New York, New York 10016

L	cake thickness (m)
L_e	experimental value of cake thickness measured at the end of filtration (m)
m	mass ratio of wet to dry cake
n	compressive coefficient
P_a	empirical constant adopted in Eqs. (17a) and (17b) (Pa)
P_L	hydraulic pressure (Pa)
P_s	solid compressive pressure (Pa)
ΔP	applied filtration pressure (Pa)
ΔP_m	pressure difference over filter medium (Pa)
q	filtration rate (m^3/m^2s)
R_m	filtration resistance of filter medium (1/m)
s	mass fraction of solids in slurry
SD	standard deviation of particle size distribution (m)
S_o	specific surface area of particles before compression (m^2/m^3)
S_o'	effective specific surface area of particles after compression, (m^2/m^3)
t	filtration time (s)
v	volume of filtrate per unit medium area (m^3/m^2)
Δw_i	mass of instantaneous cake formation per unit filtration area (kg/m^2)
x	distance from the surface of the filter septum to the cake surface (m)
δx	cake thickness change due to compression (m)
Δx	thickness of filter cake deposited in time interval Δt (m)

Greek Letters

α	specific filtration resistance (m/kg)
α_o	initial specific filtration resistance at $P_s = 0$ (m/kg)
β	exponent adopted in Eqs.(17a) and (17b)
ε	porosity of cake
ε_f	equilibrium porosity after compression adopted in Eq. (8)
μ	fluid viscosity (Pa·s)
ρ	density of fluid (kg/m^3)
ρ_s	density of particles (kg/m^3)
τ	retardation time (s)
Ω	specific surface-area ratio

Subscripts

av	average value of filter cake properties
i	filter cake properties at the cake surface, properties of a newly formed layer on the cake

j	properties of the filter-cake layer being deposited during the jth time increment, $j = 1$ *to* i
t	properties of filter cake at time t
x	local value of filter cake properties at a distance x from the filter medium

ACKNOWLEDGMENT

The authors wish to express their sincere gratitude to the National Science Council of the Republic of China for financial support.

REFERENCES

1. Tiller, F.M.; Green, T.C. The Role of Porosity in Filtration IX: Skin Effect with Highly Compressible Materials. AIChE J. **1973,** *19* (6), 1266–1269.
2. Tiller, F.M.; Yeh, C.S.; Leu, W.F. Compressibility of Particulate Structures in Relation to Thickening, Filtration, and Expression—a Review. Sep. Sci. Technol. **1987,** *22* (2&3), 1037–1063.
3. Jönsson, K.A.; Jönsson, B.T.L. Fluid Flow in Compressible Porous Media. AIChE J. **1992,** *38* (9), 1340–1348.
4. Fane, A.G.; Hodgson, P.H.; Leslie, G.L. In *Crossflow Microfiltration of Biofluids and Biomass—New Perspectives,* Proceedings for the 6th World Filtration Congress, Nagoya, Japan, May 18–21, 1993; The Society of Chemical Engineering, Japan, 5–13.
5. Tiller, F.M. The Role of Porosity in Filtration I: Numerical Methods for Constant Rate and Constant Pressure Filtration Based on Kozeny's Law. Chem. Eng. Prog. **1953,** *49* (9), 467–479.
6. Sørensen, P.B.; Hansen, J.A. Extreme Solid Compressibility in Biological Sludge Dewatering. Water Sci. Technol. **1993,** *28* (1), 133–143.
7. Shen, C.; Russel, W.B.; Auzerais, F.M. Colloidal Gel Filtration: Experiment and Theory. AIChE J. **1994,** *40* (11), 1876–1891.
8. Landman, K.A.; White, L.R.; Eberl, M. Pressure Filtration of Flocculated Suspensions. AIChE J. **1995,** *41* (7), 1687–1700.
9. Lee, D.J.; Ju, S.P.; Kwon, J.H.; Tiller, F.M. Filtration of Highly Compactible Filter Cake: Variable Internal Flow Rate. AIChE J. **2000,** *46* (1), 110–118.
10. Tosun, I. Mathematical Formulation of Cake Filtration for Deformable Solid Particles. Chem. Eng. Sci. **1985,** *40*, 673–674.
11. Akiyama, T.; Atsumi, K. Mathematical Formulation of Cake Filtration for Deformable Solid and Uniqueness of a Similarity Solution. Chem. Eng. Sci. **1987,** *42* (11), 2790–2792.

Marcel Dekker, Inc.
270 Madison Avenue, New York, New York 10016

12. Meeten, G.H. Septum Resistance and Filtration of Deformable Particles in Suspension. Chem. Eng. Sci. **2000,** *55* (1), 1755–1767.
13. Lu, W.M.; Hwang, K.J. Mechanism of Cake Formation in Constant Pressure Filtrations. Sep. Technol. **1993,** *3* (7), 122–132.
14. Lu, W.M.; Huang, Y.P.; Hwang, K.J. Methods to Determine the Relationship Between Cake Properties and Solid Compressive Pressure. Sep. Purif. Technol. **1998,** *13* (1), 9–23.
15. Lu, W.M.; Huang, Y.P.; Hwang, K.J. Dynamic Analysis on Constant Rate Filtration. J. Chem. Eng. Jpn. **1998,** *31* (6), 969–976.
16. Tiller, F.M.; Huang, C.J. Theory of Filtration Equipment. Ind. Eng. Chem. **1961,** *53* (7), 529–537.
17. Fischmeister, H.F.; Arzt, E.; Olsson, L.R. Particle Deformation and Sliding During Compaction of Spherical Powders: A Study by Quantitative Metallography. Powder Metallurgy **1978,** *4*, 179.
18. Lu, W.M.; Tung, K.L.; Hung, S.M.; Shiau, J.S.; Hwang, K.J. Compression of Deformable Gel Particles. Powder Technology **2001,** *116*, 1–12.
19. Tiller, F.M.; Shirato, M. The Role of Porosity in Filtration VI: New Definition of Filtration Resistance. AIChE J. **1964,** *10* (1), 61–67.
20. Happel, J.; Brenner, H. *Low Reynolds Number Hydrodynamics*, 2nd Ed.; Prentice-Hall: Englewood Cliffs, NJ, 1965; 395.
21. Sparrow, E.M.; Loeffler, A.L., Jr. Longitudinal Laminar Flow Between Cylinders Arranged in Regular Array. AIChE J. **1959,** *5* (3), 325–330.
22. Lu, W.M. "Theoretical and Experimental Analysis of Variable Pressure Filtration and the Effect of Side Wall Friction in Compression-Permeability Cells." (Ph.D. Diss., University of Houston, Houston, Texas, 1968).
23. Tung, K.L. "Study on the Mechanisms of Filtrations for Deformable Particles and Clogging of Filter Cloths." (Ph.D. Diss. NTU, Taipei, Taiwan, 1998).
24. Campbell, I.; Duffus, J.H. *Yeast—a Practical Approach*; IRL Press Limited: Oxford, England, 1988.
25. Ruth, B.F. Correlating Filtration Theory with Industrial Practice. Ind. Eng. Chem. **1946,** *38* (6), 564–571.

Received August 2000
Revised November 2000

Request Permission or Order Reprints Instantly!